Xavier P. Morelle
School of Engineering and Applied Sciences,
Kavli Institute for Bionano
Science and Technology,
Harvard University,
29, Oxford Street,
Cambridge, MA 02138
e-mail: morelle.xavier@gmail.com

Ruobing Bai
School of Engineering and Applied Sciences,
Kavli Institute for Bionano
Science and Technology,
Harvard University,
29, Oxford Street,
Cambridge, MA 02138
e-mail: ruobing1220@gmail.com

Zhigang Suo[1]
Fellow ASME
School of Engineering and Applied Sciences,
Kavli Institute for Bionano
Science and Technology,
Harvard University,
29, Oxford Street,
Cambridge, MA 02138
e-mail: suo@seas.harvard.edu

Localized Deformation in Plastic Liquids on Elastomers

A plastic liquid such as toothpaste and butter deforms like an elastic solid under a small stress and like a plastic solid under a large stress. Recently, plastic liquids have been used as compliant electrodes for elastomeric transducers. Here, we study the deformation of a plastic liquid adherent on an elastomer when the elastomer is stretched monotonically. We observe that deformation in the plastic liquid localized into shear bands and necks. We further observe that the plastic liquid slips near the interface between the plastic liquid and the elastomer. Each pulling edge of the plastic liquid develops a shear tail, a thin layer of the plastic liquid adherent to the elastomer. As the elastomer is stretched, the tail conforms to the deformation of the elastomer, and the plastic liquid above the tail slips. Finite element simulations confirm that localization occurs even for a relatively simple elastic–plastic model, but require a boundary condition that allows the near-interface slip. [DOI: 10.1115/1.4037410]

Introduction

Plastic liquids are all around us, from consumer products such as toothpaste, butter, and ketchup, to industrial products such as lubricants and conductive grease (Fig. 1). These materials, also known as viscoplastic fluids, soft jammed solids, and yield stress liquids, are commonly made of concentrated emulsions, colloidal suspensions, physically crosslinked gels, granular pastes, and foams [1–4]. Their rheological behavior has long been studied using shear rheometers [5–7] and extrusion channels [3,8,9]. These experimental setups closely resemble traditional applications of plastic fluids.

The growing interest in stretchable electronics, biomedical engineering, and soft lithography has motivated new applications of plastic liquids. In particular, electrically conductive plastic liquids such as carbon grease have been used as compliant electrodes. Applications include electromechanical actuators [10,11], electrical energy generators [12,13], and extension sensors [14]. In such an application, thin layers of carbon grease are spread over the surfaces of a sheet of elastomer. The plastic liquid fulfills the basic rheological requirements of the application. When the elastomer is stationary, the plastic liquid also remains stationary and does not flow and drip under gravity or small disturbance. When the elastomer undergoes large and repeated elastic deformation, the plastic liquid conforms and undergoes viscoplastic deformation.

It has been discovered recently that a plastic liquid develops a wavy pattern when the underlying elastomer is stretched *cyclically* [15]. The surface of the plastic liquid is initially flat. As the elastomer is stretched and released cyclically, a wavy pattern emerges on the surface of the plastic liquid. The wavelength remains unchanged, but the amplitude of the wave increases cycle by cycle, and then saturates after some number of cycles.

Here, we report further experiments to show that the deformation in the plastic liquid can localize even when the underlying elastomer is stretched *monotonically*. When the stretch of the elastomer is small, the deformation in the plastic liquid is homogeneous. When the stretch of the elastomer is large, the plastic liquid forms many shear bands or a single neck. Furthermore, the pulling edges of the plastic liquid develop shear tails, corresponding to large slips in the plastic liquid, parallel to and near the interface between the plastic liquid and elastomer. We conduct a finite element simulation to understand these experimental findings. We find that the near-interface slip is essential for localized deformation to occur in the plastic liquid on the elastomer. Without the slip, the deformation in the plastic liquid will not localize even when the elastomer is under a very large stretch. With the slip, the deformation in the plastic liquid will localize when the elastomer is under a similar stretch as observed in experiments.

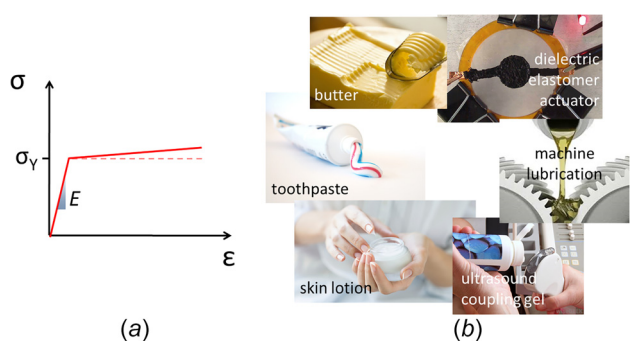

Fig. 1 (*a*) A plastic liquid deforms like an elastic solid of Young's modulus *E* when the stress is small and like a plastic solid when the stress is above the yield stress σ_Y. Some strain hardening can be observed. (*b*) Examples of applications of plastic liquids.

[1]Corresponding author.

Contributed by the Applied Mechanics Division of ASME for publication in the Journal of Applied Mechanics. Manuscript received June 27, 2017; final manuscript received July 23, 2017; published online August 18, 2017. Editor: Yonggang Huang.

 Copyright © 2017 by ASME

Downloaded From: http://appliedmechanics.asmedigitalcollection.asme.org/ on 08/21/2017 Terms of Use: http://www.asme.org/about-asme/terms-of-use

Experimental Setup

Following Ref. [15], we use lithium grease (AGS Company, Muskegon, MI, Catalog No. WL-15, Lith-Ease White) as the plastic liquid and an acrylic elastomer (3M VHB 4910) as the substrate. We have observed similar phenomena using other plastic liquids (carbon grease, toothpaste, butter, etc.). The choice of lithium grease over other plastic liquids comes from the following facts: (i) The solvent of the lithium grease is silicone oil, which evaporates negligibly at room temperature. (ii) The lithium grease has finer particles than the carbon grease does and is more uniform. (iii) The yield stress of lithium grease is high enough for the material to retain its shape under gravity, allowing us to use a vertical experimental setup. The choice of VHB over other elastomers comes from the following facts: (i) The VHB is highly stretchable, readily beyond ten times its original length. (ii) The elastic modulus of the VHB is small enough to be stretched even by hands and is much larger than the elastic modulus of the lithium grease. (iii) The adhesion between the VHB and lithium grease is strong enough to avoid debonding.

The lithium grease consists of an uncrosslinked or partially crosslinked polymer network, fine particles (e.g., lithium-containing compound, calcium carbonate, and titanium dioxide), and silicone oil (Fig. 2(*a*)) [7,16]. The stress–strain curve of the grease is close to that of an ideal elastic–plastic solid with some hardening [15] (Fig. 2(*b*)). A small rate-dependency is observed when the applied shear rate is varied over two orders of magnitude. We will not study the rate effect in the present study and will keep a constant loading rate of $\sim 0.2\,\mathrm{s}^{-1}$ in our experiments.

Care was taken to deposit flat layers of lithium grease on the surface of the VHB elastomer. To obtain a layer of the grease of a certain thickness, acrylic sheets of the corresponding thickness were placed on the surface of the elastomer as spacers. An excessive amount of the grease was first roughly placed in between those spacers on the elastomer. A razor blade was used to slide over the spacers to remove the excess of the grease. The low adhesion between the grease and the razor blade ensures flat surfaces. The layer of the grease so obtained had a root mean square roughness around 5 μm [15]. After the spacers were removed, the razor blade was used to cut the grease into rectangular shape with straight edges. We made layers of the grease of thickness H ranging from 1 to 6.5 mm, and width W ranging from 5 to 30 mm. The thickness of the elastomer was 1 mm, and its width and length were always larger than those of the grease layer.

The elastomer was then stretched up to four times its initial length, in a universal testing machine (Instron 5966) with a 50 N load cell. The deformation of the grease was videotaped with both front and lateral views (Fig. 3).

Experimental Observations

The shear modulus of the VHB elastomer ($\sim$600 kPa) [17] is much higher than that of the lithium grease ($\sim$16.6 kPa) [15]. When the stretch of the elastomer is small, the grease deforms nearly homogeneously and conforms to the deformation of the elastomer. When the stretch of the elastomer is large, the deformation of the grease becomes inhomogeneous (Fig. 4). For a specimen of a large initial width-to-thickness ratio, numerous shear bands form. For a specimen of a small initial width-to-thickness ratio, a single neck forms. We have kept $L \gg H$, such that the variation of the length of the grease does not appreciably affect localization.

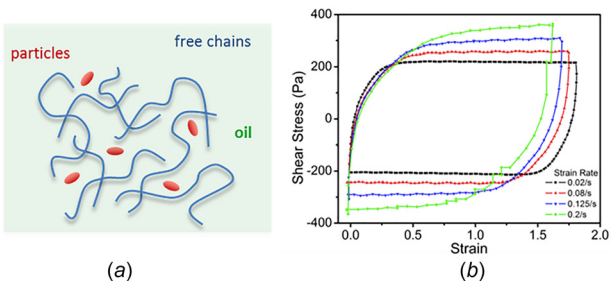

Fig. 2 (*a*) Microstructure of the lithium grease; (*b*) stress–strain curves of the lithium grease loaded at several strain rates [15]

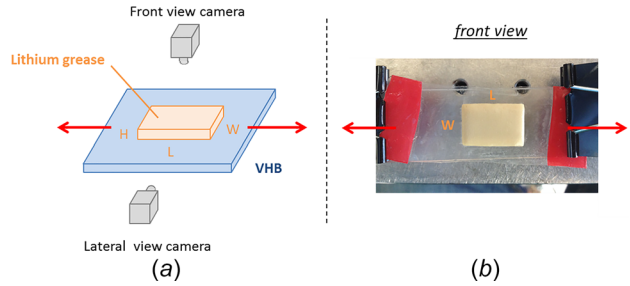

Fig. 3 Experimental setup. A schematic (*a*) and a photo (*b*) of a layer of lithium grease on a sheet of VHB elastomer. When the elastomer is stretched, the deformation in the grease is recorded by the cameras from the front and the side.

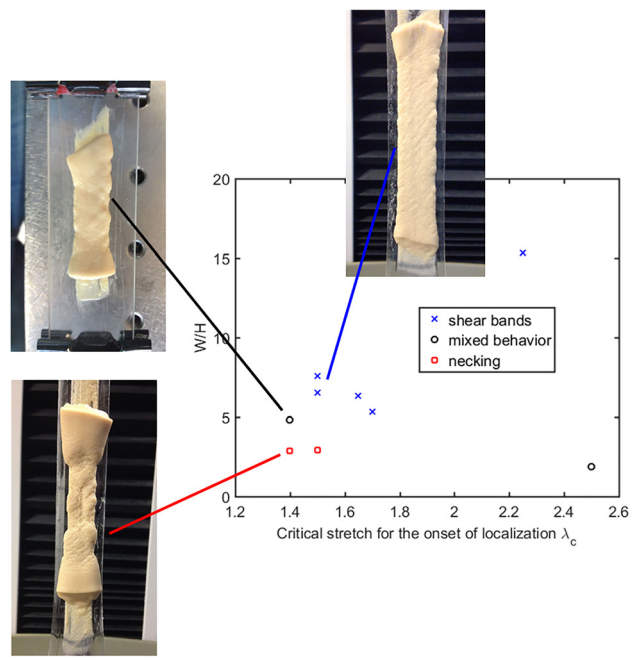

Fig. 4 When *W*/*H* is large, numerous shear bands form. When *W*/*H* is small, a single neck forms.

As noted above, for a specimen of a large width-to-thickness ratio, numerous shear bands form in the grease as the elastomer is stretched (Fig. 5). The first shear bands initiate from imperfections on the side edges or the top surface of the grease (Fig. 5(*b*)). After initiation, each shear band is thin, and runs across the width of the grease at an angle close to 45 deg (Fig. 5(*c*)). As the elastomer is stretched further, more shear bands form, soon covering the grease, with nearly even spacing. As the elastomer is stretched even further, the shear bands rotate to accommodate the reduction in the width due to Poisson's effect (Fig. 5(*d*)). The initial shear bands are thin and shallow (approximately a few tens of microns), but grow wide and deep (approximately hundreds of microns). The side edges become more and more uneven (Fig. 5(*e*)).

At the initiation stage, the distance between the first shear bands is of the order of millimeters, comparable to the initial thickness of the layer H. When the layer reaches the later stage with evenly distributed shear bands, the distance between shear bands decreases to hundreds of microns (Fig. 6). It can thus be stated

Downloaded From: http://appliedmechanics.asmedigitalcollection.asme.org/ on 08/21/2017 Terms of Use: http://www.asme.org/about-asme/terms-of-use

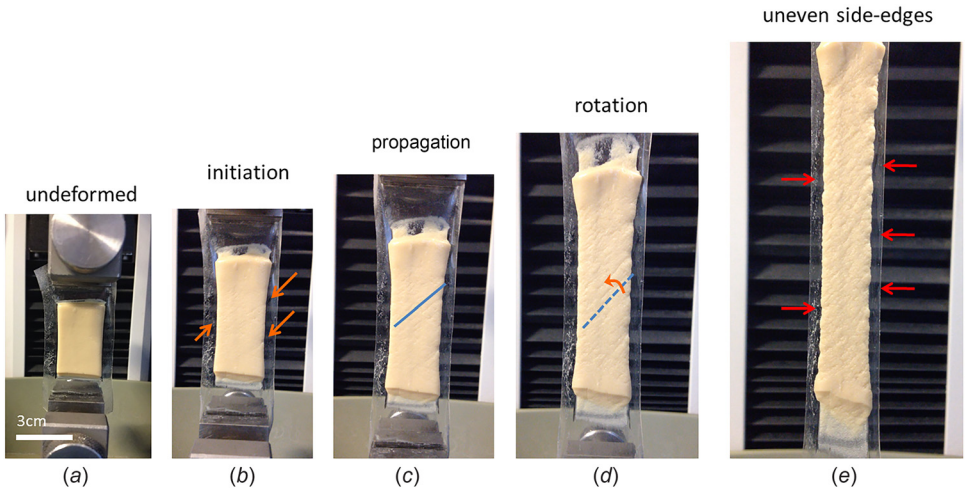

Fig. 5 The formation of shear bands in a slender plastic liquid ($W/H \geq 5$). The initial dimensions of the plastic liquid are $H = 3$ mm, $W = 22.75$ mm, and $L = 32.7$ mm.

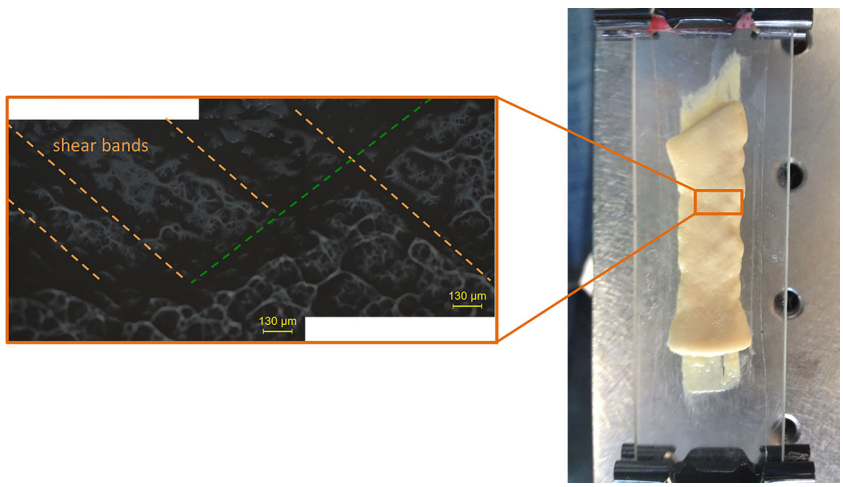

Fig. 6 Zoom-in on the surface morphology of the shear bands in an optical microscope. The initial dimensions of the lithium grease layer are $H = 6.5$ mm, $W = 31.2$ mm and $L = 23$ mm.

that the larger the applied stretch, the more the distance between shear bands is reduced, confirming an earlier observation in Ref. [15].

For a specimen of a small width-to-thickness ratio, shear bands still form, but the localization is much more strongly marked with a neck in the center of the specimen (Fig. 7). The deformation is almost solely concentrated in the neck and shows much deeper grooves (>1 mm). As the neck extends to form a significantly thinner band at larger stretch, some secondary necks form (Fig. 7(*c*)). Meanwhile, thin shear bands can still coexist with the main neck. However, bifurcation concentrates on a single localized region instead of being evenly distributed over the specimen.

In both cases, the shear bands and necks persist upon unloading and form irregular surface patterns. No significant difference was observed in terms of the critical stretch for the onset of localization ($\lambda_c = 1.71 \pm 0.39$) between the two types of localization. For layers of intermediate width-to-thickness ratios, it was observed that the two types of localization modes gave some mixed behavior (Fig. 4).

In all experiments that we have performed, each pulling edge of the grease develops a shear tail (Fig. 8). The tail is a thin layer of grease, about 100-μm thick, adherent to the elastomer. As the elastomer is stretched, the tail also deforms, conforming to the deformation of the elastomer. A block of the grease above the tail

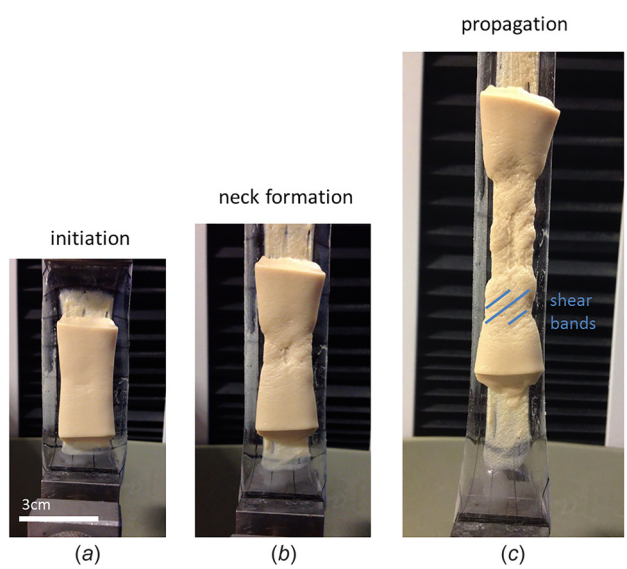

Fig. 7 The formation of neck in a plastic liquid layer ($W/H \leq 5$). The initial dimensions of the lithium grease layer are $H = 6.5$ mm, $W = 18.8$ mm, and $L = 33$ mm.

Downloaded From: http://appliedmechanics.asmedigitalcollection.asme.org/ on 08/21/2017 Terms of Use: http://www.asme.org/about-asme/terms-of-use

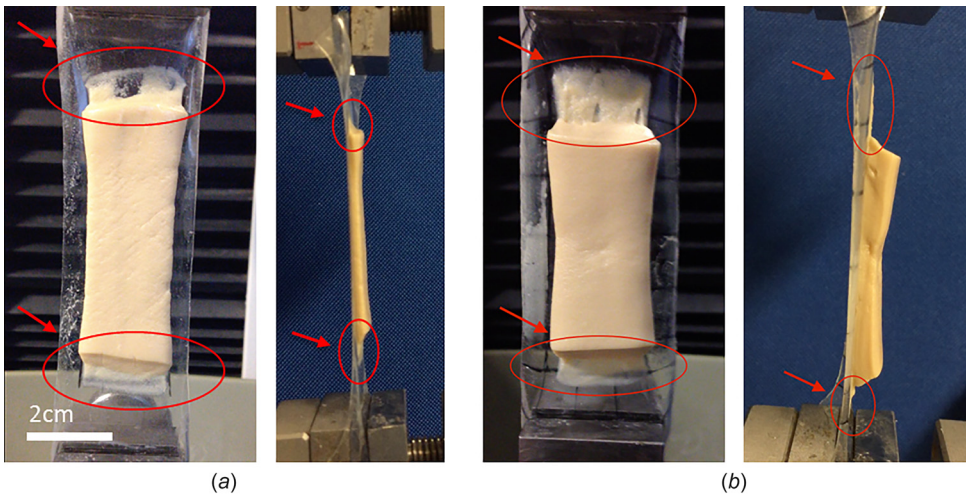

Fig. 8 The formation of shear tails. At each pulling edge of the grease, a thin layer of the grease remains adherent to the elastomer. Relative to the thin layer, a block of the grease slips. (*a*) A thin specimen ($H = 3$ mm, $W = 22.75$ mm, and $L = 32.7$ mm). (*b*) A thick specimen ($H = 6.5$ mm, $W = 18.8$ mm, and $L = 33$ mm). The side view also shows that the grease/elastomer interface remains flat.

slips relative to the tail, deforming only slightly. The middle portion of the grease, away from the two pulling edges, deforms substantially. Consequently, the grease deforms into a shape of a dumbbell (e.g., Fig. 7(*c*)).

The formation of the shear tails highlights shear localization in the grease. The thickness of the shear tail is much smaller than the initial thickness H of the grease, so that the thickness of the slipping block is approximately H. The shear stress required for slip is denoted by τ_o and the length of a slipping block by B. The bottom surface of the slipping block is subject to the shear stress τ_o, and the top surface of the slipping block is traction-free. One end of the slipping block is the edge of the grease and is traction-free. The other end of the block is connected to the middle portion of the grease and is subject to the stress at the level of the yield stress σ_Y. The forces acting on the slipping block were balanced, and we obtain that $\tau_o B = \sigma_Y H$. In the case of Fig. 7, for example, $H = 6.5$ mm, and we take the length of slipping block to be $B \approx 20$ mm, so that $\tau_o = 0.3\sigma_Y$.

Numerical Simulations

To understand the experimental findings, we conduct finite element simulations using the commercial software ABAQUS 6.12/standard. The observed localization in the grease is three-dimensional, and the rheology of the grease is not fully characterized. The detailed numerical simulation is beyond the scope of this paper. Instead, we will use an idealized model to identify basic ingredients that trigger localization.

Specifically, we simulate the plane strain deformation of a time-independent, isotropic-hardening, elastic–plastic material. Since the elastomer is far stiffer than the grease, we only simulate the grease and represent the elastomer by boundary conditions on the bottom boundary of the grease. Recalling that the experimentally observed distance between shear bands at initiation is comparable to the thickness H of the undeformed grease, we represented the undeformed layer by a rectangle of width $2H$ and height H in the simulation. To represent an initial imperfection on the top surface of the grease, we perturb the top edge of the rectangle into a sinusoidal shape, with wavelength $l = 2H$ and a small amplitude $A = 0.001H$. Similar approaches have been used to trigger surface instability in other works of the literature [15,18]. Because of symmetry, we only simulate the right half of the rectangle (Fig. 9(*a*)). The left boundary of the mesh corresponds to a line of symmetry, and the right boundary is subject to a displacement $u = u_o$, so that the applied strain is $\lambda = 1 + u_o/H$.

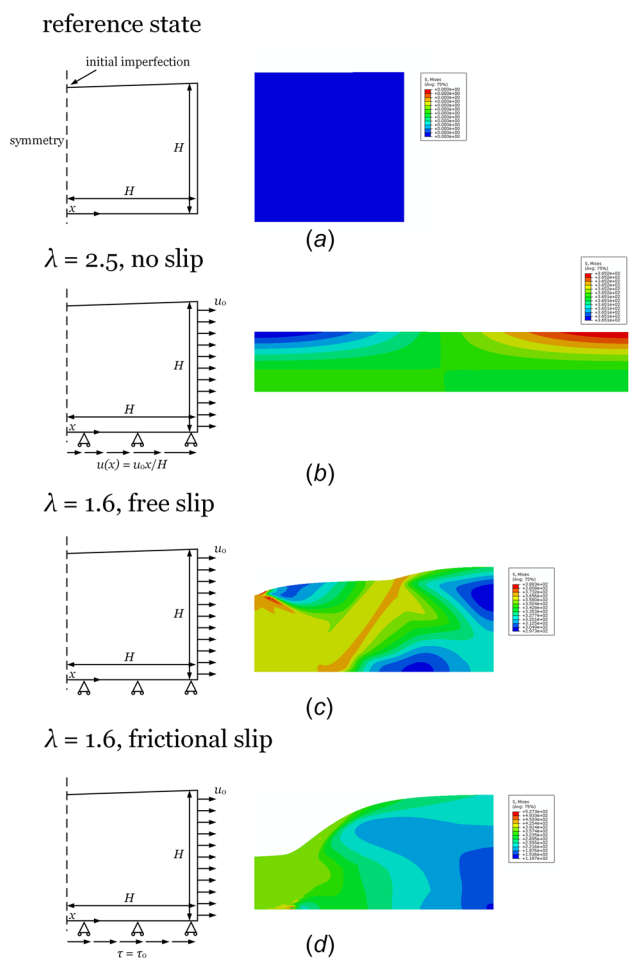

Fig. 9 The effect of boundary conditions on localization. (*a*) In the reference state, the grease is represented by a rectangle, with top surface perturbed into a sinusoidal shape. (*b*) Under the no slip condition, the deformation does not localize even at $\lambda = 2.5$. (*c*) Under the free slip condition, deformation localizes at $\lambda = 1.6$. (*d*) Under the frictional slip condition, deformation also localizes at $\lambda = 1.6$.

Downloaded From: http://appliedmechanics.asmedigitalcollection.asme.org/ on 08/21/2017 Terms of Use: http://www.asme.org/about-asme/terms-of-use

On the bottom boundary of the rectangle, we prescribe zero vertical displacement. This boundary condition comes from the experimental observation that the grease/elastomer interface remains flat. In the horizontal direction, we consider three possibilities: *no slip*, *free slip*, and *frictional slip*. In the case of no slip, we prescribe a linearly distributed horizontal displacement, $u = u_o x/H$ on the bottom boundary (Fig. 9(*b*)). In the case of free slip, we prescribed no horizontal constraints on the bottom boundary (Fig. 9(*c*)). In the case of frictional slip, we prescribed a constant distributed shear stress, $\tau = 0.3\sigma_Y$, where σ_Y is the yield strength of the material (Fig. 9(*d*)). This boundary condition is close to our estimate above of the shear stress required for slipping.

Experimentally measured stress–strain curves indicate that the grease exhibits some strain-hardening, and that the stress–strain curves are rate-dependent (Fig. 2(*b*)). The shape of the stress–strain curves motivates us to simulate the plastic liquid using a power-law isotropic-hardening, elastic–plastic model. Moreover, since all the experiments were conducted under the same strain rate, we applied a time-independent model to simplify the problem. These assumptions are typically used to simulate metals [19,20] and have also been used recently in the case of plastic liquids [15,21]. The model assumes that the material is incompressible in the plastic regime, but allows compressibility in the elastic regime. We assume yield stress $\sigma_Y = 330\,\text{Pa}$, Young's modulus $E = 50\,\text{kPa}$, and Poisson's ratio $\nu = 0.4$. In the plastic regime, the plastic liquid follows the power law $\sigma = K\varepsilon^n$ subjected to uniaxial tensile loading. Here, we considered the case of $n = 0.02$, accounting for moderate strain hardening. Comparing the power law with the yield condition $\sigma = \sigma_Y$ at $\varepsilon = \sigma_Y/E$, we obtained the hardening coefficient $K = \sigma_Y^{1-n}E^n = 365\,\text{Pa}$.

We first consider the case of no slip. Despite the initial perturbation of the top layer, no strong localization occurs even up to very large stretch $\lambda = 2.5$ (Fig. 9(*b*)). This result is consistent with that of a previous simulation [22]. Consider two materials, A and B, where A suffers localized deformation by itself, but B does not. If a thin layer of A is bonded to B, and B is sufficiently strong, B will constrain A and also prevent localization in A.

This discrepancy between this theoretical conclusion and our experimental observations is discussed as follows: The observed "shear tail" clearly indicates an inhomogeneous shear strain distribution through the thickness of the grease. Similar observations have been reported in the experiments of a plastic liquid flowing in an inclined channel [5,23]. As a consequence, the bulk part of the grease shows clear signs of sliding, while a thin boundary layer of the grease remains well bonded to the elastomer. From the experimental observations, the thickness of the boundary layer ($\sim$100 μm) is much smaller than the overall thickness of the layer (1–6.5 mm). The no-slip model fails to simulate the high shear localization between the boundary layer and the bulk layer.

Following the above discussion, we performed a second model by studying the other extreme scenario, i.e., the block of grease can slip freely. The corresponding results show the initiation of localization at a stretch of $\lambda = 1.6$ (Fig. 9(*c*)). The free slip condition is equivalent to applying tensile force to a free-standing layer. Strain-hardening elastic–plastic materials are known to form necks. Such a behavior is common for ductile metals.

Our experiments have shown that, at each pulling edge, a block of grease of a finite length slips relative to a thin layer of grease adherent to the elastomer. As noted above, this observation suggests that the slip requires a finite shear stress. We implemented a third scenario with the intermediate case, i.e., frictional slip. The effect of the boundary layer was accounted for by a constant shearing stress at the bottom, with a representative magnitude $\tau_o = 0.3\sigma_Y$. The output shows a strong single neck localization around the initial defect at a stretch of $\lambda = 1.6$ (Fig. 9(*d*)).

Conclusion

We report experimental findings of localized deformation of a plastic liquid adherent on an elastomer. When the elastomer is stretched monotonically, the plastic liquid develops shear bands and necks. Each pulling edge of the plastic liquid develops a shear tail. The tail is a thin layer of plastic liquid adherent to the elastomer, and the block of the plastic liquid above the tail slips. Finite element simulations confirm that localization can be predicted through the use of a relatively simple elastic–plastic model but requires a careful definition of the applied boundary conditions. Further study is needed to account for the full spectrum of deformation of plastic liquids on elastomers, for instance, to formulate a material model that can predict the formation and thickness of shear tails.

Funding Data

- Belgian American Educational Foundation (Cabeaux-Jacobs 2015).
- Division of Materials Research (Grant No. 14-20570).

References

[1] Bingham, E. C., 1916, "An Investigation of the Laws of Plastic Flow," Bulletin of the Bureau of Standards, Vol. 13 (Scientific Paper 278), U.S. National Bureau of Standards, Gaithersburg, MD, pp. 309–353.

[2] Larson, R. G., 1999, *The Structure and Rheology of Complex Fluids*, Oxford University Press, New York, pp. 801–802.

[3] Barnes, H. A., 1999, "The Yield Stress—A Review or '*παντα ρει*'—Everything Flows?" J. Non-Newtonian Fluid Mech., **81**(1–2), pp. 133–178.

[4] Balmforth, N. J., Frigaard, I. A., and Ovarlez, G., 2014, "Yielding to Stress: Recent Developments in Viscoplastic Fluid Mechanics," Annu. Rev. Fluid Mech., **46**(1), pp. 121–146.

[5] Ovarlez, G., Rodts, S., Chateau, X., and Coussot, P., 2009, "Phenomenology and Physical Origin of Shear Localization and Shear Banding in Complex Fluids," Rheol. Acta, **48**(8), pp. 831–844.

[6] Olmsted, P. D., 2008, "Perspectives on Shear Banding in Complex Fluids," Rheol. Acta, **47**(3), pp. 283–300.

[7] Radulescu, A. V., and Radulescu, I., 2006, "Rheological Models for Lithium and Calcium Greases," Mechanika, **59**(3), pp. 67–70.

[8] Coussot, P., 2014, "Yield Stress Fluid Flows: A Review of Experimental Data," J. Non-Newtonian Fluid Mech., **211**, pp. 31–49.

[9] German, G., and Bertola, V., 2010, "Formation of Viscoplastic Drops by Capillary Breakup," Phys. Fluids, **22**(3), p. 033101.

[10] Pelrine, R., Kornbluh, R., Pei, Q., and Joseph, J., 2000, "High-Speed Electrically Actuated Elastomers With Strain Greater Than 100%," Science, **287**(5454), pp. 836–839.

[11] Keplinger, C., Sun, J.-Y., Foo, C. C., Rothemund, P., Whitesides, G. M., and Suo, Z., 2013, "Stretchable, Transparent, Ionic Conductors," Science, **341**(6149), pp. 984–987.

[12] Pelrine, R., Kornbluh, R. D., Eckerle, J., Jeuck, P., Oh, S., Pei, Q., and Stanford, S., 2001, "Dielectric Elastomers: Generator Mode Fundamentals and Applications," Proc. SPIE, **4329**, p. 148.

[13] Koh, S. J. A., Zhao, X., and Suo, Z., 2009, "Maximal Energy That can be Converted by a Dielectric Elastomer Generator," Appl. Phys. Lett., **94**(26), p. 262902.

[14] O'Brien, B., Thode, J., Anderson, I., Calius, E., Haemmerle, E., and Xie, S., 2007, "Integrated Extension Sensor Based on Resistance and Voltage Measurement for a Dielectric Elastomer," Proc. SPIE, **6524**, p. 652415.

[15] Huang, J., Yang, J., Jin, L., Clarke, D. R., and Suo, Z., 2016, "Pattern Formation in Plastic Liquid Films on Elastomers by Ratcheting," Soft Matter, **12**(16), pp. 3820–3827.

[16] AGS-Company, 2016, "Safety Data Sheet of Lith-Ease White Lithium Grease-WL-14, WL-15," AGS-Company, Muskegon, MI, accessed Jan. 21, 2016, http://agscompany. com/images/stories/MSDS/English/White-Lithium-Lith-Ease-Grease_WL-14-15_ English.pdf

[17] 3M, 2015, "VHB™ Tape Specialty Tapes—Technical Data," 3M, London, ON, Canada, accessed Aug. 8, 2017, http://multimedia.3m.com/mws/media/1235574O/specialty-tapes-vhb-technical-data-sheet.pdf

[18] Wong, W., Guo, T.F., Zhang, Y.W., and Cheng, L., 2010, "Surface Instability Maps for Soft Materials," Soft Matter, **6**(22), pp. 5743–5750.

[19] Li, T., Huang, Z., Suo, Z., Lacour, S.P., and Wagner S., 2004, "Stretchability of Thin Metal Films on Elastomer Substrates," Appl. Phys. Lett., **85**(16), pp. 3435–3437.

[20] Lu, N., Suo, Z., and Vlassak, J. J., 2010, "The Effect of Film Thickness on the Failure Strain of Polymer-Supported Metal Films," Acta Mater., **58**(5), pp. 1679–1687.

[21] Jørgensen, L., Le Merrer, M., Delanoë-Ayari, H., and Barentin, C., 2015, "Yield Stress and Elasticity Influence on Surface Tension Measurements," Soft Matter, **11**(25), pp. 5111–5121.

[22] Li, T., Huang, Z. Y., Xi, Z. C., Lacour, S. P., Wagner, S., and Suo, Z., 2005, "Delocalizing Strain in a Thin Metal Film on a Polymer Substrate," Mech. Mater., **37**(2), pp. 261–273.

[23] Coussot, P., Raynaud, J. S., Bertrand, F., Moucheront, P., Guilbaud, J. P., Huynh, H. T., Jarny, S., and Lesueur, D., 2002, "Coexistence of Liquid and Solid Phases in Flowing Soft-Glassy Materials," Phys. Rev. Lett., **88**(21), p. 218301.

Downloaded From: http://appliedmechanics.asmedigitalcollection.asme.org/ on 08/21/2017 Terms of Use: http://www.asme.org/about-asme/terms-of-use